

# Selective Crystallization of BaF<sub>2</sub> under a Compressed Langmuir Monolayer of Behenic Acid

Lehui Lu, Haining Cui, Wei Li, Hongjie Zhang, and Shiquan Xi\*

Laboratory of Rare Earth Chemistry and Physics, Changchun Institute of Applied Chemistry, Chinese Academy of Science, Changchun 130022, China

Received May 3, 2000. Revised Manuscript Received October 5, 2000

Selective crystallization of BaF<sub>2</sub> crystals under a compressed Langmuir monolayer of behenic acid [CH<sub>3</sub>(CH<sub>2</sub>)<sub>20</sub>COOH] has been studied by using X-ray diffraction, X-ray photoelectron spectroscopy, scanning electron microscopy, and energy-dispersive X-ray analysis. It was found that, in the absence of a monolayer, three kinds of crystals (Ba<sub>2</sub>ClF<sub>3</sub>, BaClF, and BaF<sub>2</sub>) can be obtained by mixing BaCl<sub>2</sub> with a NH<sub>4</sub>F solution. However, in the presence of the monolayer of behenic acid, only BaF<sub>2</sub> crystals appear at the monolayer–subphase interface and crystals have a special crystal face (100). During this process of crystallization, the monolayer plays a very important role and acts as a template that can preferentially select a special crystal and a special crystal face. The above results can be explained in terms of a specific molecular interaction between ions and the headgroups of the monolayer and specific electrostatic, geometric, and stereochemical interactions at the organic–inorganic interface.

## Introduction

In recent years, there has been much interest in the use of organized organic assemblies as inductive templates for the controlled crystallization of both organic and inorganic crystals.<sup>1–8</sup> Previous work mainly focused on the use of Langmuir monolayers of organic surfactant as substrates for both organic and inorganic crystallization.<sup>9–28</sup> These studies have shown that the compressed

monolayers have high selectivity in the nucleation and crystal growth when two-dimensional domains in the monolayer are structurally compatible with the two-dimensional lattice of a specific crystal face. The structural compatibility appears to be largely dependent on geometric and stereochemical factors, although electrostatic interaction is also an essential element of the recognition process. For example, Tang et al.<sup>29</sup> reported the selective crystal growth between CuSO<sub>4</sub>·5H<sub>2</sub>O and Na<sub>2</sub>SO<sub>4</sub>·7H<sub>2</sub>O under a compressed monolayer. They found that between CuSO<sub>4</sub>·5H<sub>2</sub>O and Na<sub>2</sub>SO<sub>4</sub>·7H<sub>2</sub>O, although both were supersaturated, the monolayer chooses only the former to nucleate under it, and the formed crystal had a special crystal face (010). This kind of preferential selectivity of the monolayer was only observed when structural information in the monolayer was correlated with specific lattice parameters in the nascent crystal. However, earlier studies in this field have paid little attention to the mechanism of monolayer selectivity for the desired crystal from several kinds of crystals, although the selectivity of monolayers for a special crystal face of crystals has extensively been investigated, particularly when these crystals have mostly the same composition (such as Ba<sub>2</sub>ClF<sub>3</sub>, BaClF,

\* To whom correspondence should be addressed. E-mail: Xisq@public.cc.jl.cn.

(1) Landau, E. M.; Levanon, M.; Leiserowitz, L.; Lahav, M.; Sagiv, J. *Nature* **1985**, *318*, 353.

(2) Copper, S. J.; Session, R. B.; Lubetkin, S. D. *J. Am. Chem. Soc.* **1998**, *120*, 2090.

(3) Mann, S.; Heywood, B. R.; Rajam, S.; Birchall, J. D. *Nature* **1988**, *334*, 692.

(4) Bunker, B. C.; Rieke, P. C.; Tarasevich, B. J.; Campbell, A. A.; Fryxell, G. E.; Graff, G. L.; Song, L.; Liu, J.; Virden, J. W.; Mcvay, G. L. *Science* **1994**, *264*, 48.

(5) Kumar, A.; Biebuyck, H. A.; Whitesides, G. M. *Langmuir* **1994**, *10*, 1498.

(6) Frostman, L. M.; Ward, M. D. *Langmuir* **1997**, *13*, 330.

(7) Shi, H. Q.; Tsai, W. B.; Ratner, B. D. *Nature* **1999**, *398*, 593.

(8) Zhao, X. K.; Yang, J.; McCormick, L. D.; Fendler, J. H. *J. Phys. Chem.* **1992**, *96*, 9933.

(9) Mann, S.; Archibald, D. D.; Didymus, J. M.; Douglas, T.; Heywood, B. R.; Meldrum, F. C.; Reeves, N. J. *Science* **1993**, *261*, 1286.

(10) Berman, A.; Ahn, D. J.; Lio, A.; Salmeron, M.; Reichert, A.; Charych, D. *Science* **1995**, *269*, 515.

(11) Landau, E. M.; Popovitz-Biro, R.; Levanon, M.; Leiserowitz, L.; Lahav, M.; Sagiv, J. *Mol. Cryst. Liq. Cryst.* **1986**, *134*, 323.

(12) Vollhardt, D.; Retter, U. *Langmuir* **1998**, *14*, 7250.

(13) Mayya, K. S.; Patil, V.; Kumar, P. M.; Sastry, M. *Thin Solid Films* **1998**, *312*, 300.

(14) Grieser, F.; Furlong, D. N.; Lchinose, I.; Kimizuka, N. *J. Chem. Soc., Faraday Trans.* **1992**, *88* (15), 2207.

(15) Popovitz-Biro, R.; Wang, J. L.; Majewski, J.; Shavit, E.; Leiserowitz, L.; Lahav, M. *J. Am. Chem. Soc.* **1994**, *116*, 1179.

(16) Mann, S. *Nature* **1993**, *365*, 499.

(17) Ma, C. L.; Lu, H. B.; Wang, R. Z.; Zhou, L. F.; Cui, F. Z.; Qian, F. *J. Cryst. Growth* **1997**, *173*, 141.

(18) Litvin, A. L.; Valiyaveetil, S.; Kaplan, D. L.; Mann, S. *Adv. Mater.* **1997**, *9*, 124.

(19) Yan, J. P.; Meldrum, F. C.; Fendler, J. H. *J. Phys. Chem.* **1995**, *99*, 5500.

(20) Berman, A.; Charych, D. *J. Cryst. Growth* **1999**, *198–199*, 796.

(21) Zhao, X. K.; Xu, S.; Fendler, J. H. *Langmuir* **1991**, *7*, 520.

(22) Li, B.; Liu, Y.; Lu, N.; Yu, J. H.; Bai, Y. B.; Pang, W. Q.; Xu, R. R. *Langmuir* **1999**, *15*, 4837.

(23) Heywood, B. R.; Mann, S. *J. Am. Chem. Soc.* **1992**, *114*, 4681.

(24) Heywood, B. R.; Mann, S. *Langmuir* **1992**, *8*, 1492.

(25) Rajam, S.; Heywood, B. R.; Walker, J. B. A.; Mann, S. *J. Chem. Soc., Faraday Trans.* **1991**, *85* (5), 727.

(26) Landau, E. M.; Wolf, S. G.; Levanon, M.; Leiserowitz, L.; Lahav, M.; Sagiv, J. *J. Am. Chem. Soc.* **1989**, *111*, 1436.

(27) Tang, R. K.; Tai, Z. H. *Langmuir* **1997**, *13*, 5204.

(28) Tang, R. K.; Tai, Z. H.; Chao, Y. Q. *J. Chem. Soc., Dalton Trans.* **1996**, 4439.

(29) Tang, R. K.; Jiang, C. Y.; Tai, Z. H. *J. Chem. Soc., Dalton Trans.* **1997**, 4037.

and  $\text{BaF}_2$ ). However, such knowledge is essential in the field of biomineralization, separation of the desired crystal, and preparation of novel materials. Moreover, the  $\text{BaF}_2$  crystal, as a kind of new scintillation material with a short decay time and a high radiation resistance, has been widely applied to high-energy physics, nuclear medicine,  $\gamma$ -ray astronomy, etc.<sup>30</sup> Unfortunately, it is difficult for traditional preparation methods to meet the increasing technological requirement for the  $\text{BaF}_2$  crystal with tailored properties, particularly for a thin film of the  $\text{BaF}_2$  single crystal. Consequently, new synthetic strategies based on the molecular design and organized assembly are needed. On the basis of the above consideration, here we have, for the first time, studied the selective crystallization of  $\text{BaF}_2$  crystals under a compressed monolayer of behenic acid. A series of interesting results have been obtained.

### Experimental Section

Behenic acid from Fluka Chemical Co. was used as supplied. A chloroform solvent was purified by standard procedures.  $\text{NH}_4\text{F}$  (A.R.) and  $\text{BaCl}_2$  (A.R.) were purchased from Beijing Chemical Reagents Industry. Water was deionized and doubly distilled.

The experiment was performed on a KSV-5000 system. The crystal face of the samples was determined by a rotating-anode X-ray diffractometer (D/max-III A, Rigaku, Cu  $K\alpha$ ). The elemental analysis of the samples was performed by X-ray photoelectron spectroscopy (XPS; VG ESCA MKII) and energy-dispersive X-ray analysis (EDXA). The morphology of the crystals was examined by scanning electron microscopy (SEM; JXA-840).

The  $\text{BaF}_2$  supersaturated solution (supersaturated ratio  $S = 10$ ,  $\text{pH} = 8.5$ ) was prepared by mixing  $\text{NH}_4\text{F}$  and  $\text{BaCl}_2$  solutions. Then, the  $\text{BaF}_2$  supersaturated solution was filtered, and the filtrate as the subphase was transferred to the trough. A calculated quantity of behenic acid (1 mg/mL in chloroform) was spread on the surface of the freshly prepared subphase. After the chloroform was evaporated for 15 min, the monolayer was slowly and carefully compressed to the targeted pressure (25 mN/m). With the pressure held for 15 min, crystals grown under the Langmuir monolayer were transferred in the Y type to a hydrophilic glass substrate for XRD measurement and to a silicon wafer for XPS, SEM, and EDXA measurements.

### Results and Discussion

A part of the  $\text{BaF}_2$  supersaturated solution has been placed for 1.5 h in the absence of the monolayer. As a result of sedimentation, the majority of crystals were located at the bottom of the crystallization vessel. XRD analysis of these crystals showed several groups of diffraction peaks corresponding to each crystal face of  $\text{BaClF}$ ,  $\text{Ba}_2\text{ClF}_3$ , and  $\text{BaF}_2$ , respectively (Figure 1a). However, when the behenic acid monolayer was present, the induction time of crystallization was obviously reduced. Crystallization preferentially occurred at the monolayer-subphase interface. The XRD pattern of

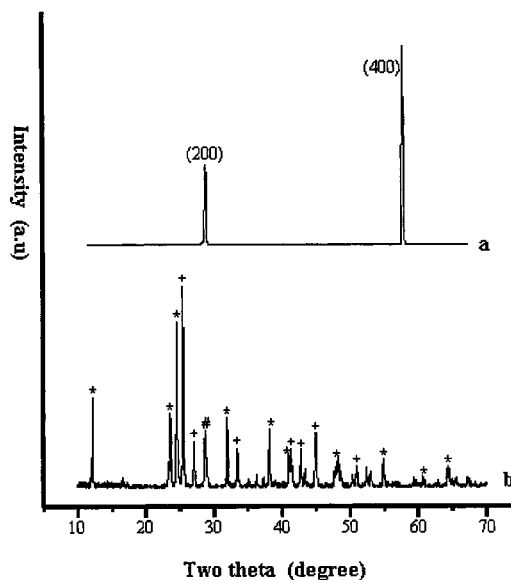


**Figure 1.** XRD image of  $\text{BaF}_2$  crystals: (a) crystals grown under the monolayer of behenic acid after 15 min; (b) crystals collected at the bottom of the vessel after 1.5 h. \* =  $\text{BaClF}$ ; + =  $\text{Ba}_2\text{F}_3\text{Cl}$ ; # =  $\text{BaF}_2$ .

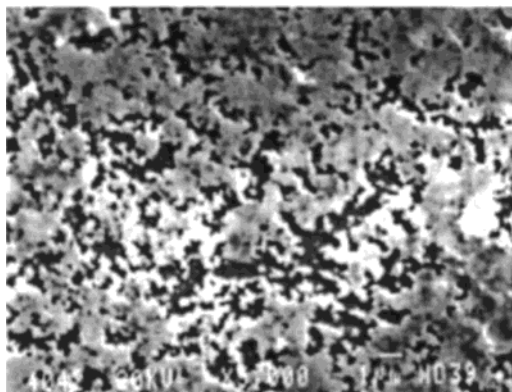


**Figure 2.** SEM micrograph of  $\text{BaF}_2$  crystals grown under the monolayer of behenic acid.

crystals grown under a behenic acid monolayer just showed the (200) and (400) reflections, thus indicating that the crystallite was (100)-oriented (Figure 1b). Viewed in SEM, the (100)-oriented crystal film was formed with a wide range of grain sizes (Figure 2). In addition, the elemental analysis of the crystal film was performed by EDXA. The EDXA pattern only showed the presence of F and Ba peaks (Figure 3). The appearance of C, Si, and Au peaks originated from the monolayer of behenic acid, silicon wafer, and Au film from the preparation of samples, respectively. This result was further confirmed by the XPS analysis. XPS measurement of crystals under the monolayer showed peaks corresponding to Ba, F, O, and C elements (Figure 4). This reveals that the (100)-oriented crystal film consists of  $\text{BaF}_2$  crystals.

The above results indicate that the presence of a behenic acid monolayer has three major effects on crystallization. First, the induction time of crystallization was reduced. Second, the behenic acid monolayer could preferentially select cubic barium fluoride, but not  $\text{BaClF}$  and  $\text{Ba}_2\text{ClF}_3$ , to nucleate under it. Third, among all of the crystal faces of  $\text{BaF}_2$ , only the (100) face was selected by the behenic acid monolayer. It is evident that

(30) Laval, M.; Moszynski, M.; Allemand, R.; Cormoreche, E.; Guinet, P.; Odru, R.; Vacher, J. *Nucl. Instrum. Methods Phys. Res.* **1983**, *206* (1-2), 169.

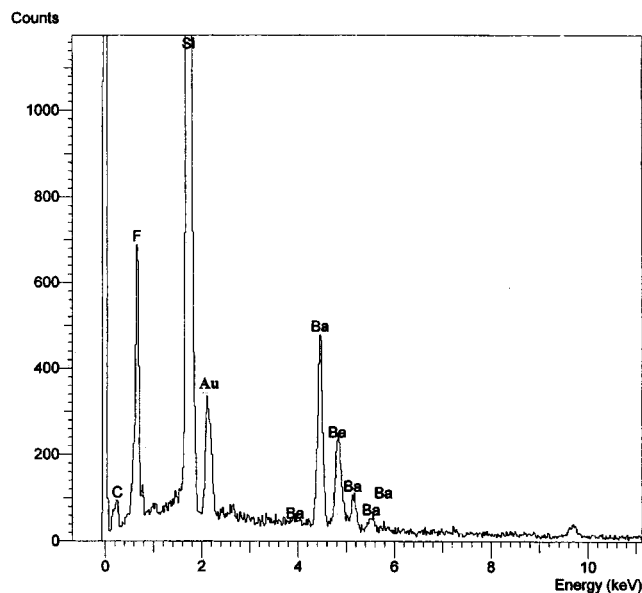


**Figure 3.** EDXA spectra recorded from crystals grown under the monolayer of behenic acid (silicon wafer).

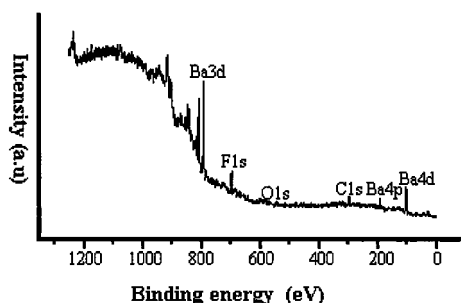


**Figure 4.** XPS spectra of BaF<sub>2</sub> crystals grown under the monolayer of behenic acid.

the behenic acid monolayer has the ability to control the oriented nucleation of inorganic crystals by geometric, electrostatic, and stereochemical interactions complementarily at the monolayer–subphase interface.

What aspects of the (100) face could be simulated by the interaction between the monolayer and BaF<sub>2</sub> crystals? Barium fluoride is known to crystallize in a cubic crystalline lattice with a lattice constant of  $a = 0.62$  nm. Atomic coordinates are (000),  $(0, \frac{1}{2}, \frac{1}{2})$ ,  $(\frac{1}{2}, 0, \frac{1}{2})$ , and  $(\frac{1}{2}, \frac{1}{2}, 0)$  for Ba atoms and  $(\frac{1}{4}, \frac{1}{4}, \frac{1}{4})$  and  $(\frac{3}{4}, \frac{3}{4}, \frac{3}{4})$  for F atoms. Drawing of the (100) projection of Ba atoms is shown in Figure 5a. The calculated distance between the closest Ba–Ba along the  $(0\bar{1}3)$  direction is 0.98 nm. On the other hand, it was reported that the compressed monolayer of fatty acid assumed hexagonal or pseudohexagonal lattices at the air–subphase interface.<sup>31,32</sup> Therefore, we deduce that the monolayer of behenic acid adopts the same packing under similar conditions (Figure 5b). Using the experimentally determined value for the surface area of one behenic acid molecule (0.204 nm<sup>2</sup>),<sup>31</sup> the lattice constant of the monolayer of behenic acid and the  $d_{(100)}$  spacing were calculated to be 0.49 and 0.42 nm, respectively. By simulation techniques, we found that superimposition of a hexagonal lattice of the

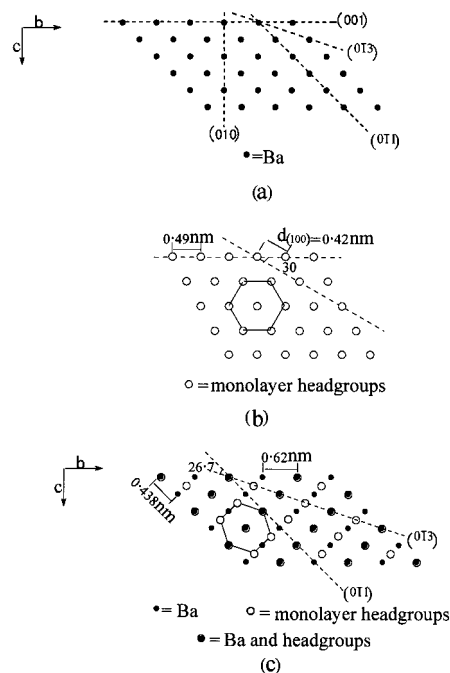


**Figure 5.** (a) Two-dimensional drawing of the (100) face of the BaF<sub>2</sub> crystal. (b) Two-dimensional packing of the monolayer headgroups. (c) Schematic representation of the proposed overlap between Ba atoms and monolayer headgroups.

headgroups of the behenic acid monolayer on the (100) face of a BaF<sub>2</sub> crystal provided only a limited geometric match (Figure 5a). The distance between the closest Ba–Ba atoms (0.438 nm) along the  $(0\bar{1}1)$  direction of the (100) face of the BaF<sub>2</sub> crystal fits the  $d_{(100)}$  plane to the network spacing of the behenic acid monolayer (0.42 nm). A comparison of the interatomic Ba–Ba distance of the (100) plane of the barium fluoride crystal (0.438 nm) with that of the  $d_{(100)}$  spacing of the behenic acid monolayer (0.42 nm) shows a mismatch of only 4%. No such relationship exists in other directions of the (100) face. However, rhombic distortion of 30° to 26.6° [the angle between  $(0\bar{1}3)$  and  $(0\bar{1}1)$ ] provides a much better matching in two dimensions. The Ba–Ba distance (0.98 nm) along the  $(01\bar{3})$  direction is 2 times that of the interheadgroup spacing (0.485 nm). A feasible arrangement is shown in Figure 5c. The figure indicates that the monolayer of behenic acid assumes a pseudohexagonal lattice at the air–subphase interface. This also implies that the pseudohexagonal packing arrangement of the monolayer of behenic acid generates a template for the oriented nucleation of BaF<sub>2</sub> crystals on the (100) face and their subsequent growth.

As far as the selectivity of the monolayer for BaF<sub>2</sub> crystals is concerned, it can be explained as follows: Previous studies indicated that a compressed surfactant monolayer adopted a definite lattice like a crystal face.<sup>3,8,31</sup> When it was spread on the surface of the subphase, the environment under the monolayer became organized, undergoing changes on physical functions such as electric field, energy and mass transmission, etc., and some other chemical functions related to the crystallization. This will account for the specific lowering of the activation energy for nucleation ( $\Delta G^*$ ) that is regarded as a function of the structure and orientation of the nuclei.<sup>29</sup> Moreover,  $\Delta G^*$  may be dependent on the two-dimensional structure of the

(31) Zasadzinski, J. A.; Viswanathan, R.; Madsen, L.; Garnæs, J.; Schwartz, D. K. *Science* **1994**, *263* (25), 1726.

(32) Dutta, P.; Peng, J. B.; Lin, B.; Ketterson, J. B.; Prakash, M.; Georgopoulos, P.; Ehrlich, S. *Phys. Rev. Lett.* **1987**, *58*, 2228.



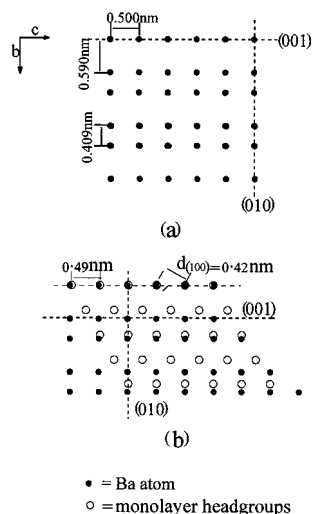


**Figure 6.** (a) Schematic representation of the packing of Ba atoms in the (100) face of the BaClF crystal. (b) Schematic diagrams showing the possible matching between monolayer headgroups and Ba atoms in the (100) face of the BaClF crystal.

different crystal faces because each set of symmetry-related faces can show a different level of complementarity with respect to the monolayer.<sup>9</sup> As for our work, there exists a good lattice matching between BaF<sub>2</sub> and the monolayer in two dimensions for the (100) face assuming a distorted hexagonal net of the monolayer. Thus, the activity energy for nucleation ( $\Delta G^*$ ), to a large extent, can be reduced because of the excellent match.<sup>4</sup> This means that the (100) face of BaF<sub>2</sub> crystals fits the behenic acid monolayer and the local environment under it. By contrast, such an excellent matching relation does not exist with respect to BaClF. For example, BaClF is tetragonal, space group  $P4/nmm$ , with unit cell dimensions  $a = 0.438$  nm and  $c = 0.722$  nm.<sup>33</sup> A comparison of the packing of Ba atoms in the (100) face of the BaClF crystal (Figure 6a) and the structures of the monolayer headgroups is given in Figure 6b. As seen in Figure 6b, a lattice match between the monolayer and the BaClF crystal occurs only along the (010) direction of the (100) face of the BaClF crystal. The coplanar Ba–Ba distance (0.500 nm) along the (010) direction of the (100) face is close to the lattice constant of the monolayer (0.49 nm). However, the Ba–Ba distance (0.590 nm) in the (001) direction of the face

(100) of the BaClF crystal is significantly larger than the corresponding spacing (0.42 nm) of the monolayer headgroups (29% misfit). Similar mismatching also exists for other crystal faces of the BaClF crystal. Additionally, the BaClF crystal<sup>34</sup> is itself unstable in solution and tends to decompose into BaCl<sub>2</sub> and BaF<sub>2</sub>. As for the Ba<sub>2</sub>ClF<sub>3</sub> crystal,<sup>33</sup> its crystal lattice is rhombohedral with  $a = 0.114$  nm and  $\alpha = 107^\circ 20'$ . Up to now, little work has been reported with more detailed data for the Ba<sub>2</sub>ClF<sub>3</sub> crystal structure. Hence, we only deduce that significant mismatching probably exists between the monolayer and the Ba<sub>2</sub>ClF<sub>3</sub> crystal according to the similar reports.<sup>8,17,23</sup> On the basis of the above analysis, we consider that, because of the good matching relationship between the monolayer and the BaF<sub>2</sub> crystals, the monolayer as a inductive “template” will first bind Ba<sup>2+</sup> ions to the carboxylate headgroups and thus stimulate preferential nucleation of BaF<sub>2</sub>, but not BaClF and Ba<sub>2</sub>ClF<sub>3</sub> crystals, under it, although BaClF and Ba<sub>2</sub>ClF<sub>3</sub> are kinetically favored in the absence of the behenic acid monolayer.

### Conclusion

The above studies have shown that the monolayer of behenic acid can preferentially select not only a special crystal (BaF<sub>2</sub>) but also a special crystal face (100). This selectivity is closely associated with a series of molecular recognition events which rely upon the translation of detailed structural information at the organic–inorganic interface; electrostatic, geometric, and stereochemical factors are key elements of this process. Undoubtedly, our present work gives an important implication for the understanding of the biomineral mechanism. It shows that the integration of supermolecular self-assembly, organized molecular film, and inorganic material chemistry provides the opportunity to develop novel synthetic strategies to select a certain crystal from the mixture and a product with uniform crystal shape-tailored morphologies and crystallographic orientation. By synthesis of proper monolayer materials, some practical application might be achieved in the future.

**Acknowledgment.** We thank Prof. Siyuan Zhang and Dr. Shan Gao for useful suggestions. We also thank the National Natural Science Foundation of China for financial support.

CM000365I

(33) Fessenden, E.; Lewin, S. Z. *J. Am. Chem. Soc.* **1995**, *77*, 4221.

(34) *CRC Handbook of Chemistry and Physics*, 58th ed.; Weast, R. C., Ed.; CRC Press: Boca Raton, FL, p B-92.